

HIGH PERFORMANCE MULTILAYER NOTCH OPTICAL FILTERS FOR HIGH ENERGY DETECTOR APPLICATIONS AND THEIR COATING PROCESS CONTROL^a

S. MALTEZOS, E. FOKITIS, D. KOUZIS-LOUKAS AND R. LIAROKAPI

*Physics Department, National Technical University of Athens,
9, Heroon Polytechniou, Zografos,
GR 15780, Athens, GREECE
E-mail: maltezos@central.ntua.gr*

High-performance and precision multilayer notch optical filters, designed and optimized to be used in high energy detector applications, are presented. As two typical examples, we present filters operating in the near UV and far UV range for air-fluorescence and RICH detectors, respectively. A proposed, improved coating process algorithm of optical monitoring during the fabrication of such filters has been developed and simulated. A prototype spectrograph equipped with fast readout electronics has been developed, aiming to be used for the thin film layer control in deposition plants.

1. Introduction

In the High Energy detectors optical filters are often used and constitute a significant component, performing optical noise rejection. As typical examples, we first describe a filter for recording the air-fluorescence, occurring during the Extensive Air Shower (EAS) in Ultra High Energy Cosmic Ray (UHECR) events. This radiation is emitted mostly from ionized molecular nitrogen (N_2^+) in discrete lines in the near UV region. In order to improve the trigger efficiency and extending the duty cycle of the fluorescence telescopes, the optical filters used must display high performances. Notch-type multilayer thin film filters [1] have been designed and simulated for the fluorescence detector of the AUGER Project [2] and could be considered for other future experiments, such as, TA [3] and EUSO [4,5]. Secondly, we describe new type of filters in the far UV range, for Fabry-Perot interferometry proposed to be used in conjunction with RICH detectors [6]. These have been designed according the detailed structure of certain parts of interest in a Pt-Ne Hollow Cathode lamp spectrum. The idea behind this approach is to maximize the signal-to-noise ratio and simplify the interferometer data analysis, in comparison to the case of using monochromator.

^a Work partially supported by research program PAVE 1994 from GSRT of Greece.

In addition, since in both cases the fabrication of the filters needs a very accurate thin film layer thickness control, and therefore filter manufacturers consider such task as state-of-the-art, we propose an improved coating process algorithm in order to aid the production of first prototypes.

2. The designed multilayer filters

For the design of a notch-type filter of non-quarterwave thickness intelligent optimization techniques are used. The “Simulated Annealing” (SA) [7] method is effective in the cases of large number of free parameters and has been successfully used for non-quarterwave multilayer filter design [8,9].

The filters used for recording the air-fluorescence must have sufficiently high transmittance in the spectral range of interest (near UV) and steep in its edges. In addition, the design must aim at reducing the optical noise, apart in the visible, also in the UV range between the peaks of transmittance. The filter we designed has two main pass-bands corresponding to the strongest group of nitrogen lines (see Ref. [1]), consisting of 20 pairs of high index: Ta_2O_5 , and low index: SiO_2 of non-quarterwave layers. on a typical UV glass substrate.

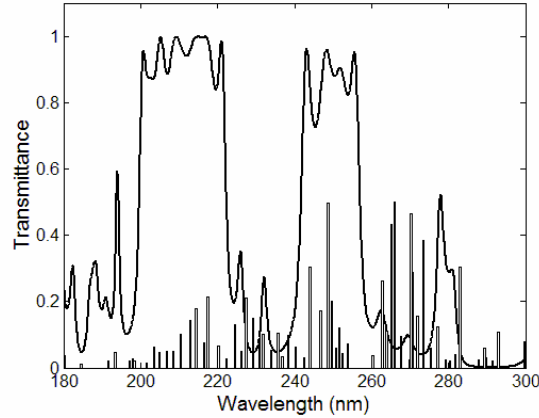


Figure 1. The spectral transmittance of the designed 80-layer notch filters for Fabry-Perot interferometry. The achieved band peaks match with the main emitted line groups of the hollow cathode lamp, as shown in the same plot.

In High Energy experiments the RICH detectors are used for charged particle identification. An appropriate gas radiator has to be used for high

momentum range. The particle velocity, β , is determined from the Cherenkov radiation angle, θ_c , and the refractive index n , and thus, a precise measurement of the refractivity ($n-1$) is necessary. This can be accomplished using a pressure tunable Fabry-Perot refractometer. A Pt-Ne hollow cathode discharge lamp can be used combined with a notch filter having two pass bands: The first band covers the shorter wavelengths in the range 200–222 nm and the second in the range 242–257 nm including another group of strong lines in longer wavelengths. This simulated filter consists from 40 pairs of high index: Al_2O_3 and low index: MgF_2 as coating materials on a SiO_2 substrate. The spectral transmittance of this filter is shown in Figure 1.

3. Coating process control method

3.1. The process control algorithm

The thickness of each deposited layer can be controlled during the deposition process with a certain accuracy using the wideband optical monitoring [10-12]. During the coating process the transmittance (or reflectance) spectral profile varies with the time because of the increasing thickness. The degree of closeness between the measured curve and the simulated one can be evaluated using a formulation of Calculus of Variation theory, using the term η -proximity [13]. In our algorithm we use the criteria of “ η -proximity of zero order” (f_0) and also the “ η -proximity of first order” (f_1), which, for i^{th} layer are defined as follows:

$$f_{0,i}(d, \lambda) = |T_{s,i}(\lambda, d_i) - T_{m,i}(\lambda, d)| < \eta_1 \quad (1)$$

$$f_{1,i}^d(d, \lambda) = \left| \frac{\partial T_{s,i}}{\partial d} \bigg|_{d_i} - \frac{\partial T_{m,i}}{\partial d} \right| < \eta_2 \quad (2)$$

$$f_{1,i}^\lambda(d, \lambda) = \left| \frac{\partial T_{s,i}}{\partial \lambda} - \frac{\partial T_{m,i}}{\partial \lambda} \right| < \eta_3 \quad (3)$$

where, d_i is the designed thickness of the i^{th} of total number M of layers,

d is the actual (running) thickness of the i^{th} layer,

$T_{m,i}(\lambda, d)$ is the measured transmittance during running thickness,

$T_{s,i}(\lambda, d_i)$ is the simulated transmittance at the designed thickness, and

η_1 , η_2 and η_3 are given positive numbers to be selected

The partial derivatives of the measured transmittance with respect to d and λ have to be calculated by a line fit along some points (i.e. the last 5) reducing the effect of their fluctuations due to co-existing noise. We define a merit function (MF), $f_i(d)$, as a function of the running thickness d , expressing the closeness of the two curves. This function is based on the sum of the average of the particular functions $f_{0,i}$, $f_{1,i}^d$ and $f_{1,i}^\lambda$ along the given points (N) written as follows:

$$f_i(d) = \frac{w_0}{N} \sum_{j=1}^N f_{0,i}(d, \lambda_j) + \frac{w_1^d}{N} \sum_{j=1}^N f_{1,i}^d(d, \lambda_j) + \frac{w_1^\lambda}{N} \sum_{j=1}^N f_{1,i}^\lambda(d, \lambda_j) \quad (4)$$

where w_0 , w_1^λ and w_1^d are weighting factors, normalized to unity, and are used for balancing the contribution of the three terms in Eq. (4) and can be optimized running the simulation program of coating process. Therefore, the overall required criterion is $f_i(d) < \eta_{av}$, where η_{av} is the weighted average of η_1 , η_2 and η_3 , using the aforementioned weight factors. The value of η_{av} depends mainly on the overall experimental systematic uncertainties and has to be determined empirically for the particular deposition plant. The prediction of the turning point in the $d, f_i(d)$ diagram can be done following two steps: a) Checking if the value of $f_i(d)$ is within a given uncertainty zone, and b) Finding the intersection point between the fitted line of the 5 recent points of f_i and the η_{av} -level horizontal line.

During the coating process, the merit function $f_i(d)$, will take its minimum value (theoretically less than η) when the running (actual) thickness d is very close to the desired one d_i . Because the parameter affecting the transmittance is the optical thickness, defined as $p_i = n_i d_i$, any deviation of n_i can be compensated by a corresponding variation of d during the coating. The achievement of this minimum leads to the decision to stop the deposition for the current material.

3.2. Spectrograph for optical monitoring

The optical monitoring can be accomplished during the layer coating by a computer controlled spectrograph. For practical reasons (such as the evaluation requirements and cost minimization), we developed a prototype spectrograph operating, not in UV but in visible region using a halogen lamp at about 5300 K. This is based on a concave holographic aberration-reduced grating, 95 mm in diameter. The grating has 792.8 grooves per mm operating in the spectral region from 380 to 780 nm (400 nm overall range) corresponding to 66.62 mm detector length, leading to a “reciprocal linear dispersion” (RLD) of 4.5 nm. The detector covers the grating spatial range and is an array of 38 silicon photodiodes with

high speed response, sensitive from the UV to near infrared region, DIP-type: S4114-38Q^b. The pitch of the element is 1 mm wide and corresponds to a fraction of the total area $38/66.62=0.5704$ leading to a partial spectral range of $0.5704 \times 400 \text{ nm} = 228.16 \text{ nm}$. Therefore, the pitch of the element corresponds to 6.0 nm in the spectral range. Locating the detector in the centre of the focal plane we obtain a total spectral range from 465.92 nm to 694.08 nm.

3.3. Readout electronics

The readout electronics consists of a commercial driver/amplifier card, type C2334-38S^b, which performs the signal multiplexing and amplifying and also of a home-made electronic system. The latter aims to convert the analogue multiplexed voltage level signals, induced from a 38-element photodiode array to digital one. An operational diagram using the fundamental blocks of the readout electronics of the spectrograph is shown in Figure 2. Timing signals for C2334 are created by a microprocessor and are in synchronization with the A/D timing signals. The digital data from the A/D are being buffered and transferred simultaneously to the PC-type computer via microprocessor's internal UART and a MAX232 serial interface.

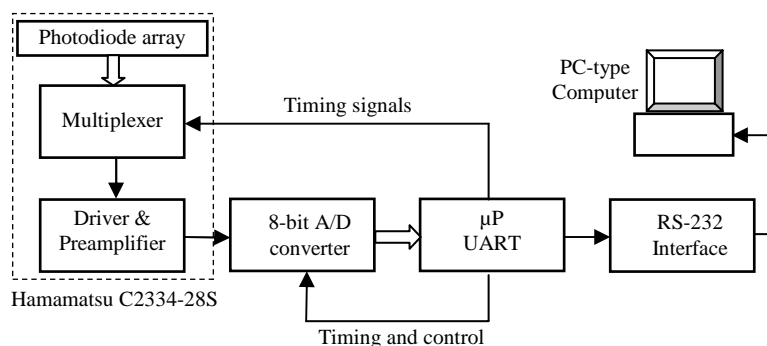


Figure 2. The operational diagram of the whole readout electronics. The commercial card has been combined with the home-made processing circuit.

Using assembly programming we achieve very high performance in the reading rate, that is, 300 spectrum images per second, which is the maximum

^b Hamamatsu Photonics K.K., Solid State Division, 1126-1 Ichino-cho, Japan

rate allowed by the commercial card. The data acquisition is controlled by a program written in LabVIEW^c environment which could be used for the coating process control proposed. In this case the theoretical transmittance curves can be pre-calculated for each deposited layer and be available for the control criteria.

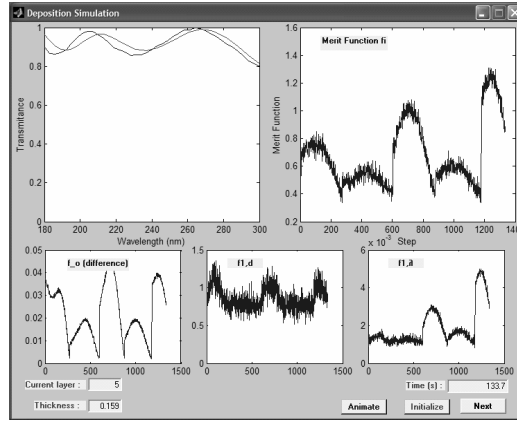


Figure 3. The panel appeared by the coating simulation program for the 80-layer Fabry-Perot filter during the coating of the first five layers.

4. Coating process simulation

Simulation of the coating process control has been developed and performed in MATLAB^d for both types of filters based on the proposed process algorithm. In this computer program we assumed to have a similar geometry and spectral resolution with that achieving by the Spectrometer, but operating in the UV region: from 180 to 180+228.16, that is 408.16 nm. In Figure 3 the evolution in time of the three terms of Eq. (4) (lower plots) and MF (upper right) are shown. The current transmittance (black curve) includes 1% noise and varies during coating of the 5th layer approaching the theoretical one (gray curve). The obtained transmittance is still far from the expected after completing the 80 layers. Running the simulation program we found that the term $f_{1,i}^d$ has higher stability without offset and with clear minima. As a result, much higher weight (w_1^d) has to be given to this term in the calculation of MF.

^c National Instruments, USA

^d MATLAB: The language of Technical Computing

5. Conclusions

The presented high-performance optical filters could be fabricated and be applied in High Energy detectors, since the technology of thin films has continued to advance and provides the required accuracy. The proposed process control algorithm seems to be stable and could be combined with an optical monitoring apparatus. The proposed process control refers to demanding in precision filter for High Energy applications. The present spectrograph is optimized for the visible and near UV range. We are considering re-designing it for application of coating including far UV range. We are looking forward to find cooperation with a research center, having an appropriate coating plant, for producing prototypes of filters presented in this paper. Part of the monitoring and control could be done with the spectrograph described.

References

1. S. Maltezos, E. Fokitis, P. Moyssides, A. Geranios, *Nucl. Phys. B (Proc. Suppl.)*, **125** (2003).
2. Auger Collaboration, *Pierre Auger Project Design Report* (1996)
3. TA collaboration, *Design report* (2000).
4. S. Bottai, G. D'Ali Staiti, M.C. Maccarone, T. Mineo, *Proc. 28th ICRC*, **Vol. HE**, (2003) (<http://www.euso-mission.org/>).
5. G. Corti, E. Pace, "Concept study of UV filters for EUSO", Report (2003).
6. T.A. Filippas, E. Fokitis, S. Maltezos, K. Patrinos, M. Davenport, *Nucl.Instr. and Meth. B*, **196** (2002).
7. Laarhoven P. J. M. and E. H. L. Aarts E. H. L., *Simulated Annealing: Theory and Applications*, *Kluwer Academic Publishers* (1992)
8. T. Boudet, P. Chaton, L. Herault, G. Gonon, L. Jouanet, and P. Keller, *Appl. Optics* **Vol. 35**, No. 31. (1978).
9. E. Fokitis, S. Maltezos, and E. Papantonopoulos, *Journal of High Energy Physics (JHEP)*, **045**, (1999).
10. B. Vidal, A. Fornier, and E. Pelletier, *Appl. Optics* **Vol. 17**, No. 7 (1978).
11. B. Vidal, A. Fornier, and E. Pelletier, *Appl. Optics* **Vol. 18**, No. 22 (1979).
12. Li Li and Yi-hsun Yen, *Appl. Optics* **Vol. 28**, No. 14 (1989).
13. A. N. Kounadis, "Elements in Calculus of Variations", NTUA, Athens (1984).